32nd URSI GASS, Montreal, 19–26 August 2017

Propagation Measurements and Modeling Techniques for 3.5 GHz Radar-LTE Spectrum Sharing

Christopher R. Anderson(1) and Gregory D. Durgin(2)
(1) Wireless Measurements Group, Electrical and Computer Engineering Department
United States Naval Academy, Annapolis MD USA
(2) The Propagation Group, Electrical and Computer Engineering Department
Georgia Institute of Technology, Atlanta, GA USA

Abstract

In the United States, government and commercial entities have begun sharing the 3550–3650 MHz military Radar band. The key to ensuring successful sharing is robust interference prediction based on accurate and reliable propagation models. This paper presents the results of a comprehensive propagation measurement and modeling campaign for the 3.5 GHz band. Although existing propagation models are broadly applicable, each one falls short in characterizing the measured propagation in this band. Using simple, openly available geographic information systems data, we have developed a modeling framework that can significantly reduce the measurement-to-model median and Root Mean Square errors.

1 Introduction

In the United States, the 3550–3650 MHz frequency band was recently authorized for spectrum sharing applications between commercial users and military Radar and satellite services [1]. The key enabler for this transformative technology will be fast, efficient, high-fidelity propagation models that produce reliable predictions even when users are rapidly moving through a complex propagation environment.

Much of the published work investigating 3.5 GHz propagation has come from researchers in Europe investigating the applicability of existing channel models to 3.5 GHz WiMax deployments, for example [2, 3, 4]. These researchers have typically focused on examining the applicability of empirical propagation models, such as Log-Distance [5], Hata-Like Models, such as the Extended Hata [6] or Stanford University Interim (SUI) [7], and semi-deterministic models, such as the Irregular Terrain Model (ITM; also known as the Longley-Rice) or the Terrain Integrated Rough Earth Model (TIREM) [8]. We observed in the literature that: (i) campaigns have focused on sub-5 km distances, which are extremely short for characterizing high-power/long-distance Radar propagation, (ii) modeling error is highly variable and can be extremely high with > 20 dB Root Mean Square Error (RMSE), and (iii) measurements have characterized propagation over relatively flat environments and have generally not taken large-scale terrain effects into account. Though known to be imperfect, the Extended Hata and ITM models are currently authorized for propagation prediction for 3.5 GHz spectrum sharing systems [9].

One of the primary drawbacks of all these models is their extremely coarse categorization of propagation environments, essentially binning them into urban, suburban, and rural. Modern Geographic Information Systems (GIS) can distinguish among dozens, and sometimes hundreds, of land use and land cover categories, all of which can be defined with highly precise geographic boundaries. Although in the context of radiowave propagation many of these environments overlap significantly, it has been widely acknowledged that utilizing a broader diversity of categories could provide a more accurate propagation prediction. A considerable amount of research has demonstrated that approximately 7–10 categories are sufficient for characterizing the local clutter environment [10]. For our modeling effort, we have chosen to use the U.S. National Land Cover Database, a 30 meter resolution raster image of 20 partially overlapping land categories [11].

2 Experimental Setup

To characterize 3.5 GHz propagation, a series of Received Signal Strength (RSS) measurements was recorded in and around St. Inigoes, Maryland, USA. A high-power SPN-43 Radar located at the U.S. Navy's Webster Field Annex was used as the transmitter, with the parameters given in [12]. The SPN-43 antenna was a horizontally polarized parabolic dish antenna installed on a rotating pedestal approximately 7.9 m above ground level. The antenna had a cosecant-squared pattern with a gain of 32 dBi and a 3 dB azimuthal beamwidth of 3°.

A block diagram of the measurement system is given in Fig. 1. For all measurements, a horizontally-polarized dipole antenna was mounted on the roof of a vehicle, approximately 2.0 m above ground level. A bandpass filter was constructed from a MiniCircuits VHF-1810 high-pass filter and VLF-4400 low-pass filter. A Herotek limiter was used

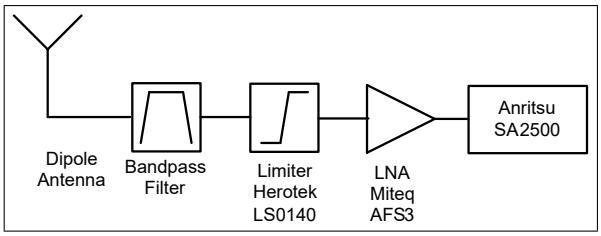

Figure 1. Block diagram of the RSS measurement system

to protect the measurement system from high-power signals expected at locations near the Radar. A Miteq AFS3 Ultra Low Noise Amplifier was used to ensure the system could record extremely weak signals at long ranges. The receiver was a Tektronix SA2500 Real-Time Spectrum Analyzer with on-board GPS. For approximately 75% of the measurements, the vehicle was moving at speeds ranging from 10–55 miles per hour (4.5–24.6 m/s); the remaining measurements were collected while the vehicle was stationary. The amplifier gains, as well as all cable/connector losses, were measured on a Vector Network Analyzer and subtracted from the recorded RSS measurements.

To record measurements, the SA2500 was configured to operate in the time-domain (Amplitude *vs.* Time) mode with a measurement bandwidth of 5.0 MHz. To mitigate the effects of the very narrow antenna beamwidth and the antenna rotation for each measurement, the SA2500 captured a 20 msec segment of data (approximately 20 Radar pulses) in max hold mode. The max hold was maintained for approximately 1 sec. as the Radar beam swept overhead before the net captured trace was saved to disk. This procedure ensured that the maximum RSS was captured as the Radar signal swept over each measurement site; however, it introduced a small uncertainty in the absolute position of the measurement, due to the movement of the vehicle[1]. For each measurement, the system also recorded GPS latitude and longitude. Postprocessing extracted the strongest RSS value from each captured data trace and used it as the RSS for that specific measurement location.

Approximately 70% of the measurements were recorded on publicly accessible areas, with the remaining measurements recorded inside the 1,000-acre Webster Field Annex. Measurements were primarily recorded either on roadways or parking lots, although to ensure a representative sampling of the region, a small number of measurements were recorded in diverse areas such as a decommissioned runway, along a beach, and off-road locations.

3 Results

Although numerous techniques exist for analyzing propagation measurements, an extremely common method used in the literature is to compute the *excess path loss*,

[1]The worst-case position uncertainty is 25 meters at the maximum vehicle speed of 55 MPH (24.6 m/s).

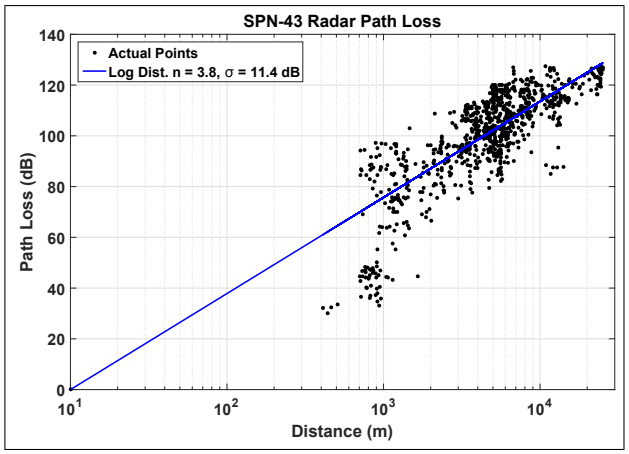

Figure 2. Scatterplot of of the 3.5 GHz propagation measurements in and around St. Inigoes, MD. Large-scale path loss calculated using Eq. (1) where the $PL(d_0)$ anchor point is the free-space path loss at a distance of 10 meters from the transmitter.

$$PL(d) = P_R(d_0) - P_R(d) \quad \text{dB}, \tag{1}$$

where $PL(d)$ is the path loss at a transmitter-receiver distance of d meters, $P_R(d)$ is the RSS recorded at a distance d from the transmitter, and $P_R(d_0)$ is either the RSS recorded at a close-in reference distance d_0 meters from the transmitter or the calculated free-space path loss at a distance of d_0. For our measurement scenario, hazardous electromagnetic radiation safety rules precluded us from making a boresight measurement at a distance closer than 120 meters. Thus, we chose to use a calculated free-space $P_R(d_0)$ at $d_0 = 10$ meters and then extract out the SPN-43 and dipole antenna gains as a function of their measured elevation pattern. This provided us with results that would have been obtained if isotropic antenna elements had been installed on the transmitter and receiver.

As shown in Fig. 2, we observed a path loss exponent of $n = 3.8$, which is suggestive of plane-earth or two-ray type propagation. We also observed a significant spread about the median path loss up to a distance of approximately 2.0 km. The spread is a result of the unique clutter environment immediately around the transmitter. To the east/northeast of the transmitter, the area is open, with few or no obstructions to block the Line of Sight (LOS) path from transmitter to receiver. Approximately 1 km to the north and south of the transmitter were several buildings with heights slightly lower than the SPN-43 antenna. The region is a mature forest with tree heights in the range of 10–12 m, with forest areas interspersed with 2- and 3-story-tall buildings that significantly attenuated the received signal.

Table 1 lists the mean and RMSE error between the Log-Distance, SUI, Extended Hata, ITM (in point-to-point mode), and TIREM models when applied to our path loss results. For ITM and TIREM, commercially available implementations of the algorithms were used, along with

Table 1. Comparison of 3.5 GHz Propagation Model Accuracy

Error	Log Dist.	Ext. Hata	Ext. SUI	ITM	TIREM	GIS Model
Mean	0.0	6.2	-24.1	3.8	-12.8	0.0
RMS	11.4	12.8	27.3	28.4	20.2	10.7
Mean $d > 2$ km	0.9	7.4	-25.6	-9.9	-13.4	0.0
RMS $d > 2$ km	10.1	12.6	27.7	18.6	19.8	9.0

All errors are reported in dB. Mean Error is calculated as $Measured - Model$

freely available 30 meter USGS Digital Elevation Maps (DEM).

Table 1 shows that the Log-Distance model provides the best overall fit to the measured data. This result makes sense, as the Log-Distance model is essentially a linear regression on the measured dataset. Examining the other models, the ITM and Extended Hata models both produce a relatively small mean error but have nearly double the variability of the Log-Distance model. TIREM and SUI have very large mean and RMS errors, with the SUI being the worst fit of all compared models. We note that our measurement scenario did not match the explicit assumptions of either the SUI or Extended Hata models. The Extended Hata presumes a transmitter height of at least 20 m and is intended for very long range (1–100 km) predictions [6]. The SUI model presumes a transmitter height of 15–40 meters, receiver heights of 2–10 meters, and distances less than 10 km. ITM and TIREM are both designed for long range propagation over hilly or rugged terrain and are not a good match for the flat terrain within the first 2–3 km of our transmitter's range.

4 GIS Propagation Modeling Framework

The general form of nearly all empirical propagation models is given as

$$\overline{PL}(d) = PL_{Base}(d) + \sum_i \Delta_i \quad \text{dB}, \tag{2}$$

where $\overline{PL}(d)$ is the median path loss (dB) as a function of the straight-line Euclidian distance d between transmitter and receiver, and $PL_{Base}(d)$ is the baseline propagation model. Δ_i represents additional attenuation factors not accounted for in the baseline propagation model, and are functions of aspects of the environment. Note that $PL_{Base}(d)$ can be any empirical or semi-empirical propagation model, although the choice of the baseline model will impact the types and values of the additional attenuation factors. Typical choices for Δ_i are factors for terrain roughness, foliage, and environmental clutter.

For our propagation modeling approach, we chose to use the log-distance model as our baseline propagation model, with two Δ_i's: one to account for the effects of terrain diffraction and one to account for receiver endpoint clutter. Although many formulations of knife-edge diffraction exist in the literature, we chose to implement a simple saturated exponential model of the form

$$L_{Diff} = D_T \left(1 - exp\left(-\frac{d_T}{d_c}\right)\right) \quad \text{dB}, \tag{3}$$

where d_T is the distance that the most significant terrain obstruction extends above the straight-line path between transmitter and receiver (meters), d_c is the terrain obstruction distance for which attenuation is saturated (m), and D_T is a tunable loss parameter that represents the maximum amount of diffraction for a given frequency and environment type (rugged mountains, rolling hills, etc.). The advantage of this approach is that it provides fast, efficient diffraction calculations while still being physically motivated and tied to physical geometry.

To categorize receiver endpoint clutter, we first downselected the 20 partially overlapping National Land Cover Data (NLCD) categories into a set of seven distinct categories, as listed in Table 2. To determine the clutter category, we analyzed only those pixels within a 200 meter radius around each receiver position[2]. Clutter categories were set based on a majority of pixels in the analyzed area, with the exception of the Rural Forest and Suburban Forest, where the majority had to be either the Rural or Suburban category with at least 25% in the NLCD "Forest" Types (41, 42, 43, or 90).

Table 2. Endpoint clutter categories based on the NLCD database

Clutter Category	NLCD Land Type	Median Atten. (dB)
Barren	11,12, 71, 72, 73, 74	N/A
Rural	21, 51, 52, 81, 82, 95	2.6
Rural Forest	Rural + 41, 42, 43, 90	-1.8
Suburban	22	9.6
Sub. Forest	Suburban + 41, 42, 43, 90	-0.5
Urban	23	7.7
Dense Urban	24	N/A

[2] 200 meters was empirically determined as the minimum radius necessary to consistently characterize similar type environments regardless of the receiver's location on the NLCD map.

5 Results

Model parameters were generated using the joint optimization approach presented in [13]. Median attenuation values for clutter categories in our measurement dataset are given in 2; additionally $D_T = 0.5$ dB and $d_c = 0.25$ m. A summary of the model performance is provided in Table 1. From our results we observe: (i) terrain diffraction in this environment has only a minor impact on the total propagation loss and is essentially a binary effect, (ii) counter-intuitive negative losses for the two forested clutter categories, and (iii) a 0.7 dB reduction in the RMS error as compared to the Log-Distance model for all distances and a 1.1 dB reduction in the RMS error for distances greater than 2.0 km.

Finally, we note that *negative* clutter loss does not imply gain; rather, it suggests that propagation in those environments is less attenuated than would be predicted by the baseline propagation model. In general, forest environments heavily attenuate wireless signals, but we observed the opposite effect in our model. Our hypothesis for this result is that, because most of our measurements were taken on highways, the signal from the SPN-43 Radar propagated over the forest canopy and then diffracted over the forest edge before reaching our receiver. The lack of significant terrain diffraction in our environment is not completely unexpected; the vast majority of the region around the SPN-43 is gently undulating terrain, with a single ridgeline to the east with a maximum height of 60 m. Only 35% of our measurements experienced any terrain diffraction at all, with geometries that would not have produced significant shadowing.

6 Conclusions

Analysis of 3.5 GHz propagation measurements in Southern Maryland demonstrated that existing propagation models do not precisely and reliably describe propagation in this band, particularly for regions that include foliage or building clutter. However, the relatively high propagation losses suggest that secondary users may be able to operate with significantly smaller exclusion zones and still avoid interference to/from S-band Radars. We demonstrated that even a simple GIS-based propagation model can provide a significant improvement in propagation modeling accuracy.

7 Acknowledgement

The authors would like to thank M. A. Lanoue, A. P. Hill, K. Butch, C. Nelson, and S. Ha for providing significant help collecting the data. This work was sponsored in part by Google and the Office of Naval Research.

References

[1] "Amendment of the Commissions Rules with Regard to Commercial Operations in the 3550-3650 MHz Band ," Tech. Rep. FCC 15-47, April 2015.

[2] W. Joseph, L. Roelens, and L. Martens, "Path Loss Model for Wireless Applications at 3500 MHz," in *Int. Symp. on Antennas and Propagation*, July 2006, pp. 4751 – 4754.

[3] N. Rakesh and D. Nalineswari, "Comprehensive performance analysis of path loss models on GSM 940 MHz and IEEE 802.16 WiMax F3.5 GHz on different terrains," in *Int. Conf. on Computer Communication and Informatics*, January 2015, p. Digest of Papers.

[4] S. A. T. K. L. Chee and T. Kürner, "Foliage attenuation over mixed terrains in rural areas for broadband wireless access at 3.5 GHz," *IEEE Trans. Antennas Propag.*, vol. 59, no. 7, pp. 2698–2706, July 2011.

[5] T. S. Rappaport, *Wireless Communications: Principles and Practice*, 2nd ed. New Jersey: Prentice Hall, 2002.

[6] E. Drocella, J. Richards, R. Sole, F. Najmy, A. Lundy, and P. McKenna, "3.5 GHz exclusion zone analyses and methodology," Tech. Rep. TR-15-510, 2014.

[7] V. Erceg, L. J. Greenstein, S. Y. Tjandra, S. R. Parkoff, A. Gupta, B. Kulic, A. A. Julius, and R. Bianchi, "An empirically based path loss model for wireless channels in suburban environments," *IEEE J. on Sel. Areas Commun.*, vol. 17, pp. 1205–1211, July 1999.

[8] D. Eppink and W. Kuebler, "TIREM/SEM HANDBOOK," Tech. Rep. ECAC-HDBK-93-076, 1994, available online at http://handle.dtic.mil/100.2/ADA296913.

[9] "Citizens Broadband Radio Service," Tech. Rep. US CFR Title 47, Chapter 1, Subchapter D, Part 96, July 2016.

[10] "The ILLR Computer Program," Tech. Rep. FCC OET-72, July 2002.

[11] (2016, April) National Land Cover Database (NLCD). [Online]. Available: https://www.mrlc.gov/nlcd2011.php

[12] F. H. Sanders, J. E. Carroll, G. A. Sanders, and L. S. Cohen, "Measurements of selected Naval Radar emissions for electromagnetic compatibility analyses," Tech. Rep. NTIA TR-15-510, October 2014.

[13] G. Durgin, T. S. Rappaport, and H. Xu, "Measurements and models for radio path loss and penetration loss in and around homes and trees at 5.85 ghz," *IEEE Trans. Commun.*, vol. 46, no. 11, pp. 1484–1496, Nov 1998.